Chain Morphologies in Semicrystalline Polyfluorene: Evidence from Raman Scattering

M. Arif, C. Volz, and S. Guha*

Department of Physics and Astronomy, University of Missouri, Columbia, Missouri 65211, USA

(Received 28 September 2005; published 19 January 2006)

The β phase in di-octyl substituted polyfluorene (PF8) exhibits a surprising level of conformational order at nanometer length scales compared to other phases. We present Raman scattering studies of PF8 as a function of thermal cycling, which establishes a connection between the conformational isomers and the side and main chain morphology. Density-functional calculations of the vibrational spectra of single chain oligomers in conjunction with the experimental results demonstrate the incompatibility of the β phase with the overall α crystalline phase in PF8.

DOI: 10.1103/PhysRevLett.96.025503 PACS numbers: 61.50.Ks, 61.41.+e, 78.30.Jw

Conjugated polymers (CPs) are now a core constituent in numerous organic and organic-inorganic hybrid technologies [1]. Polyfluorenes (PFs) have emerged as an especially attractive CP family due to their strong blue emission, high charge mobility, excellent chemical and thermal stability, and thus great prospects for device applications [2,3]. Almost all PF derivatives utilize solubilizing side chain substituents anchored at the bridging carbon atom (see Fig. 1) to mold the explicit molecular level properties. These side chains give rise to a rich array of mesomorphic behavior with the appearance of a nematic liquid crystalline (n-LC) phase, which renders facile uniaxial orientation resulting in polarized light emission [4,5]. There are many ambiguities regarding chain conformations and crystalline phases in PFs. Vibrational frequencies and intensities determined by Raman spectroscopy are strongly influenced by variations in the chain planarity as well as side chain conformations. Application of Raman scattering is particularly useful in PFs for discerning the families of chain conformers and structural phases.

Specifically in the PFs there is evidence of local inhomogeneities in the structural order that give rise to heuristic families of conformation isomers with, in sum, both segmental and wormlike disorder [6]. A prime example is poly (di-n-octylfluorene) (PF8) in which a low energy emitting β chromophore, proposed to originate in regions of enhanced chain planarity [7], reflects a surprising level of conformational order over short distances compared to other phases and conformations. The optical properties of PF8 are extremely sensitive to the exact film forming conditions and thermal history [8]. This is in stark contrast to branched PFs such as (2-ethyl)hexylfluorene (PF2/6) in which there is a single ensemble average distribution in the chain conformations. Thus, the optical absorption and emission properties of PF2/6 are relatively insensitive to the exact crystallographic state. This ‘‘homogeneous’’ heterogeneity is reflected in the Raman spectrum of PF2/6 as well, which is rather insensitive to temperature, structural phase or processing history [9]. PF8 therefore constitutes an almost unique ‘‘test’’ case in which to further extend the analysis of Raman scattering to include monomers with differing main and side chain conformations.

The focus of this Letter is on chain morphologies in PF8. Using Raman spectroscopy, we show that the β phase critically depends on the di-octyl chain conformation. To our knowledge, this is the first time light scattering techniques are used for identification of this chromophore. To understand the exact origin of the β phase, PF8 must be assessed in terms of both the distribution of conformational isomers as well as its crystalline phase. Our experimental Raman scattering results of PF8 as a function of thermal cycling in conjunction with first-principles theoretical vibrational spectra calculations of fluorene oligomers with varying torsional angles and side chain conformations demonstrate the incompatibility of the β phase with the α crystalline phase.

Structural studies of PF8 have identified at least five crystalline phases, schematically shown in Fig. 1(d). In addition to an n-LC mesophase appearing at temperatures above 150 °C, two crystalline phases (α and α') have been isolated, which are seen upon cooling from the n-LC state at different levels of undercooling [10]. Additionally, several conformational isomers have been identified in PF8

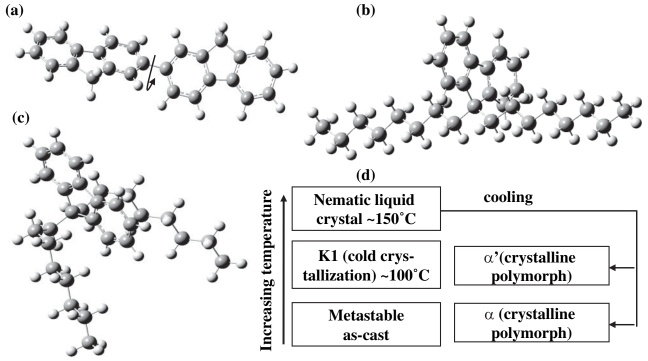

FIG. 1. (a) Sketch of a fluorene dimer, and di-octyl substituted fluorene monomer with (b) all *anti* conformation and (c) *anti-gauche-gauche* conformation of the alkyl side chain. (d) Schematic of the crystalline phases in PF8.

depending upon the torsional angles between the fluorene monomers, shown by the arrow in Fig. 1(a). The β phase is one such conformational isomer that represents a more planar backbone conformation and is identified in spectroscopic measurements as a separate long wavelength feature in both optical absorption and emission spectra [5,7]. Although this phase appears as a minority constituent, it dominates the optical emission [8].

The PF8 sample was obtained from American Dye Source (BE-129) and used either as received or dissolved in *p*-xylene and dried. The Raman spectra were collected by an Invia Renishaw spectrometer attached to a confocal microscope with a ×50 long objective and a 785 nm line of a diode laser as the excitation wavelength. The samples were affixed to a stainless steel sample holder of a Linkam LTS350 microscope hot-cold stage.

All theoretical computations of the fluorene oligomers were performed with hybrid density-functional theory in the GAUSSIAN03 [11] program. We employed the B3LYP (Becke's three parameter hybrid) functional [12] to perform geometry optimization and calculations of force constants, dipole moments, and polarizability derivatives combined with the polarized 3-21G* basis set. Other basis sets such as the 6-31G or 6-311G yield comparable frequencies but often give unsatisfactory Raman intensities [13]. Table I compares our calculated unscaled Raman frequencies of five strong peaks of a fluorene monomer using the 3-21G* and 6-311G* basis sets with the experimental values [14]. Cuff and Kertesz have shown that the 3-21G basis set within the scaled quantum mechanical oligomer force field method yields excellent agreement between experimental and theoretical vibrational spectra of fluorene and poly(*p*-phenylene) [15].

The Raman frequencies were calculated from fluorene monomers for two limiting conformations of the *n*-octyl side chains: an all *anti*-alkyl side chain (aaa) [Fig. 1(b)] and an *anti*-*gauche*-*gauche* (agg) side chain conformation [Fig. 1(c)]. Vibrational frequencies of a fluorene dimer and trimer (with no side chain substitution) were calculated by varying the torsional angle between the monomers as test cases for conformational isomers of PF8. Because the GAUSSIAN code calculates only frequency-independent Raman activities, it is necessary to correct for the frequency dependence of the scattering intensity, described in greater detail in Ref. [16]. All calculated frequencies reported are unscaled, normalized to the C-C intraring stretch frequency at 1600 cm^{-1}, and have been broadened with a Lorentzian line shape of full width at half maximum (FWHM) of 10 cm^{-1}.

TABLE I. Experimental frequencies of five intense Raman peaks of a fluorene crystal. The second and third columns show the calculated Raman frequencies (cm^{-1}) of a fluorene monomer using different basis sets.

Expt. Freq. (cm^{-1})[a]	3-21G*	6-311G*
1610	1634	1650
1478	1483	1484
1234	1251	1261
1022	1051	1047
738	765	763

[a] Reference [14].

The Raman frequencies in the 1250–1350 cm^{-1} region are mainly associated with the backbone C-C stretch mode [17]. Figure 2 shows the experimental spectra at different temperatures. The top spectrum taken at room temperature (RT) after cooling the sample from the *n*-LC phase is representative of the α crystalline phase. The 1257 and 1280 cm^{-1} peaks originate from a combination of C-H bending and C-C stretching motion of the bond connecting the two phenyl rings within the monomer; the former is particularly sensitive to the torsional angle between the neighboring monomer units. The 1307 cm^{-1} peak represents the C-C stretch mode between adjacent monomer units. The 1350 cm^{-1} peak experimentally observed is the C-C stretch motion from within the monomer unit; in fluorene oligomers this peak is hardened by almost 20 cm^{-1} as seen in our calculated Raman spectra of the monomer, dimer, and trimer.

A recent modeling study by Chunwaschirasiri *et al.* [18] has identified three different conformational isomers in terms of the local polyfluorene backbone torsional angle: C_α, C_β, and C_γ that reflect the PF8 chain structure at very short length scales. C_β, conventionally referred to as the β phase, is the more planar form with a torsional angle ~165°; C_α and C_γ are associated with torsional angles of 135° and 155°, respectively. In order to simulate the β phase, we calculated the Raman spectrum of the oligomers where the angle between adjacent monomers was fixed at 180°. (Geometry optimization of the oligomers yield a torsional angle of ~138° which reflects the C_α conformer.) Figure 2 shows our calculated Raman spectra for an opti-

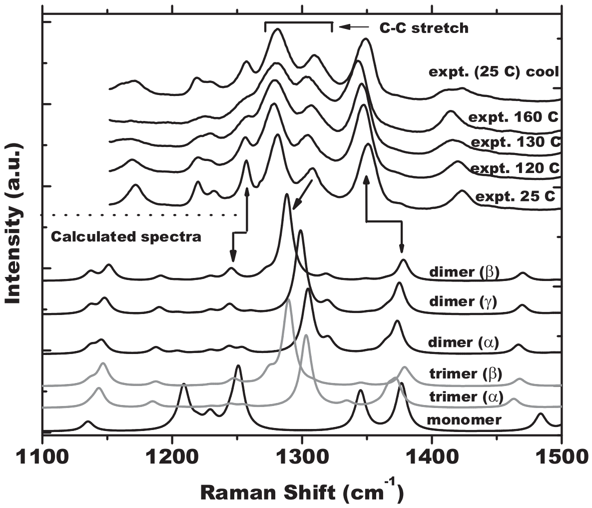

FIG. 2. The top five show the experimental Raman spectra at various temperatures. Calculated Raman spectra of a fluorene monomer, timer, and dimer are shown below for varying torsion angles.

mized monomer, and trimer and dimer with varying torsion angles (C_α, C_β, and C_γ isomers). The monomer has additional peaks in the 1200 cm^{-1} region that mainly arise as a combination of the squeezing motion of the carbon atoms of the phenyl rings and C-H bending motion. The C-C stretch mode between the adjacent monomers (~1305 cm^{-1}) softens by almost 16 cm^{-1} for the C_β dimer. (Note that this is completely absent in the monomer.) A similar trend is observed for the C_β trimer. The frequency position of this C-C stretch mode can thus be used as a test bench for the presence of C_β conformers.

The as-is PF8 sample has a high fraction of the C_β conformer, which was ascertained by the presence of the 437 nm peak in the absorption spectrum of a thin film of the sample [5]. Figure 3(a) inset shows the peak position of the 1307 cm^{-1} as a function of heating and cooling. With increasing temperatures the Raman frequency positions typically decrease due to a decrease in the intermolecular and intramolecular quasielastic force constants. A striking feature is the enhancement of the frequency position of this peak by more than 3 cm^{-1} at 130 °C. This reflects a transformation of the C_β conformers to the C_α and C_γ conformers, consistent with our theoretical calculations (Fig. 2) where the 1307 cm^{-1} peak position is significantly enhanced for the α conformer compared to the planar β conformer in a dimer or trimer. We point out that the C_β conformer has a torsional angle ~165°; hence, we expect a smaller shift in the Raman frequency from the C_β to the C_α or C_γ conformers compared to our theoretical calculations where we held the β phase at 180°. Upon cooling one observes a linear increase in the frequency positions, typically observed in crystalline solids. Owing to a long-range three-dimensional ordering, hardening of frequencies in PF8 upon cooling reflect the contraction of the ordered (semi)crystalline phase.

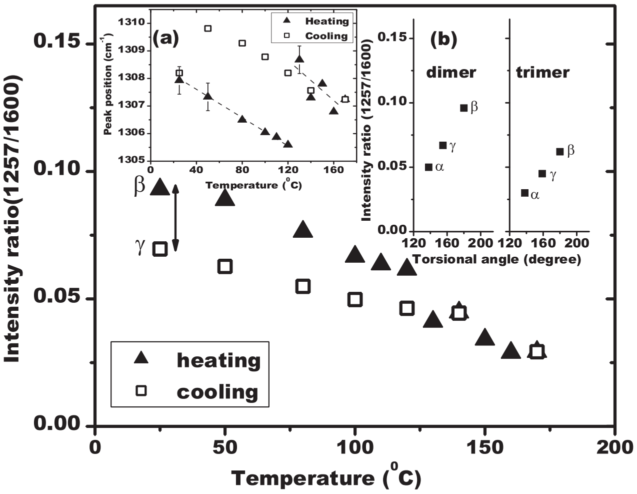

FIG. 3. Intensity ratio of the 1257 cm^{-1} to the 1600 cm^{-1} peak vs temperature both during the heating and cooling cycle. Inset (a) shows the peak position of the 1307 cm^{-1} Raman peak as a function of temperature. Inset (b) is the calculated I_{1257}/I_{1600} ratio of a dimer and a trimer for varying torsional angles.

The 1257 cm^{-1} peak is highly sensitive to temperature, which is again a manifestation of transformation of the conformers. The peak intensity is normalized to the 1600 cm^{-1} peak (I_{1257}/I_{1600}); this ratio decreases with increasing temperatures and upon cooling the sample back to RT the intensity is ~26% less compared to the as-is sample, as shown in Fig. 3. Our calculated I_{1257}/I_{1600} ratio in the dimer and trimer [Fig. 3(b)] as a function of the torsional angles shows a similar trend; a 30%–35% difference is observed between the C_γ and C_β chromophore. We interpret our experimental result as a transformation of the C_β chromophore to C_γ or C_α upon heating the sample. Upon cooling, the polymer chains most probably have a large fraction of the C_γ chromophore observed from the experimental and calculated I_{1257}/I_{1600} ratio. Additionally, the 1308 cm^{-1} appears at a slightly higher frequency upon cooling it back to RT [Fig. 3(a)] consistent with our calculations where the C_γ chromophore has a higher frequency compared to C_β.

The presence of the β phase in PF8 is strongly coupled to the overall crystalline phase of the polymer and conformation of the side chains at nanometer length scales. Upon warming and thermal cycling of the polymer, new Raman peaks appear and distinct changes in the Raman spectra occur that can be explained on the basis of specific conformation of the alkyl side chains. Next, we focus on the issue of ordering and conformation of the alkyl side chain and its consequence on the torsional angles.

Side chain conformation as a function of the crystalline phase can be further probed by studying the low frequency region (100–700 cm^{-1}) of the Raman spectra. Local ordering in n-alkanes going from the solid state to the melt at ~32 °C, particularly evolution of intramolecular and intermolecular structures with temperature has been studied by many groups in the past three decades [19,20]. An accepted picture in n-alkanes upon heating is that the crystallization goes through the formation of seeds consisting of weakly bundled segments of transplanar chains with short segments (8-9 CH_2 segments) [21]. In PFs the complexity arises from an interdependence of side chain ordering to the polymer backbone conformation.

The top two spectra in Fig. 4 are the experimental Raman spectra of the as-is and the α crystalline sample in the low frequency region. The bottom three are the calculated spectra of the aaa and agg side chain substituted fluorene monomer. The 420 cm^{-1} peak observed in our calculations is the ring torsional mode (as deciphered from the displacement pattern), which is observed at a slightly higher frequency ~480 cm^{-1} in the polymer. This peak is seen at 480 cm^{-1} in all PFs with varying side chains and is almost temperature insensitive, making it a viable candidate for the ring torsional mode. The strong 275 cm^{-1} peak in the fluorene monomer is mainly the out of plane motion of the hydrogens attached to the bridging carbon, which, of

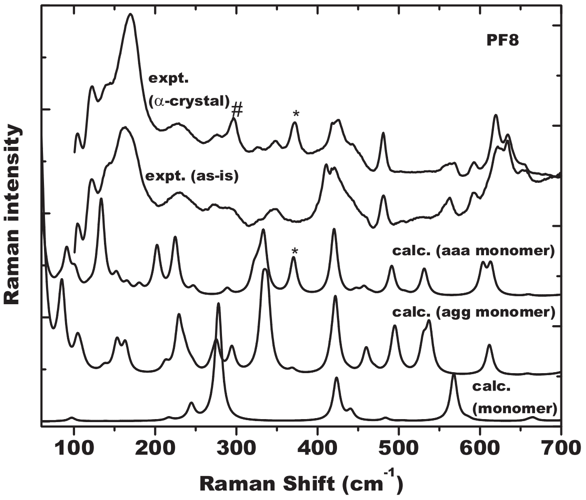

FIG. 4. Raman spectra of as-is and α crystalline PF8 in the low frequency region (top two). The bottom three spectra are the calculated Raman spectra of a fluorene monomer, and fluorene monomer with agg and all aaa chain conformations.

course, is absent in the side chain substituted monomer. Two new peaks at 290 and 370 cm^{-1}, marked by symbols in Fig. 4, in the α crystalline (thermally cycled) sample are observed. The latter can be explained in terms of the all *anti* conformation of the alkyl side chain.

Strong LAM (longitudinal accordion motion) modes in *anti* planar *n*-alkanes occur at low frequencies; in nonadecane LAM1 and LAM3 modes appear at 125 and 342 cm^{-1}, respectively [19]. The calculated spectrum of the aaa conformer clearly shows the LAM3 mode at 370 cm^{-1}, which is totally absent in the agg conformer. The appearance of the 370 cm^{-1} peak and the enhancement of the 140 cm^{-1} region in the α crystalline phase of PF8 is a clear indication of all *anti* conformation of the alkyl side chain in this phase. These results establish a connection between side chain ordering and the local conformations.

The work by Chunwaschirasiri *et al.* [18] shows that the presence of the C_β conformer is possible only when the alkyl side chains adopt an agg-type conformation. Based on this and our theoretical vibrational spectra calculations, we can understand why the β phase is incompatible with the α crystalline phase. This a direct consequence of the conformation of the alkyl side chains, which adopts an aaa conformation in the α crystalline phase of PF8. Additionally, the appearance of the 290 cm^{-1} Raman peak in the α crystalline phase is most probably the rocking motion of the bridging carbon in the C_α or the C_γ chromophore. This agrees with our dimer or trimer calculations where this rocking motion is seen at 250 cm^{-1} only for a nonplanar conformation of the molecule.

In conclusion, we have shown experimental evidence of the incompatibility of the C_β chromophore with the overall α crystalline phase in PF8. This is attributed to a large scale increase in the population of *anti* planar conformation of the alkyl side chains. Our studies were based on combined theoretical vibrational spectra calculations of single chains in conjunction with experimental Raman scattering studies. Such studies are an important step towards developing a universal picture of structure-property relationship in CPs that mainly derive from chain morphology at short length scales.

S. G. acknowledges the donors of the American Chemical Society Petroleum Research Fund, the University of Missouri Research Board, and the National Science Foundation (DMR-0413601 and ECS-0523656) for partial support of this work. We have greatly benefited from fruitful discussions with Michael Winokur and Marilia Caldas.

---

*Corresponding author.
Electronic address: guhas@missouri.edu

[1] F. J. M. Hoeben, P. Jonkheijm, E. W. Meijer, and A. P. H. J. Schenning, Chem. Rev. **105**, 1491 (2005).
[2] M. Leclerc, J. Polym. Sci., Part A **39**, 2867 (2001).
[3] U. Scherf and E. J. W. List, Adv. Mater. **14**, 477 (2002).
[4] D. Neher, Macromol. Rapid Commun. **22**, 1365 (2001).
[5] M. Grell, D. D. C. Bradley, G. Ungar, J. Hill, and K. S. Whitehead, Macromolecules **32**, 5810 (1999).
[6] M. Knaapila, R. Stepanyan, M. Torkkeli, B. P. Lyons, T. P. Ikonen, L. Almasy, J. P. Foreman, R. Serimaa, R. Güntner, U. Scherf, and A. P. Monkman, Phys. Rev. E **71**, 041802 (2005).
[7] A. J. Cadby, P. A. Lane, H. Mellor, S. J. Martin, M. Grell, C. Giebeler, D. D. C. Bradley, M. Wohlgenannt, C. An, and Z. V. Vardeny, Phys. Rev. B **62**, 15 604 (2000).
[8] M. J. Winokur, J. Slinker, and D. L. Huber, Phys. Rev. B **67**, 184106 (2003).
[9] B. Tanto, S. Guha, C. M. Martin, U. Scherf, and M. J. Winokur, Macromolecules **37**, 9438 (2004).
[10] S. H. Chen, A. C. Su, C. H. Su, and S. A. Chen, Macromolecules **38**, 379 (2005).
[11] GAUSSIAN 03, Gaussian, Inc., Pittsburgh, PA, 2003.
[12] A. D. Becke, J. Chem. Phys. **98**, 5648 (1993).
[13] D. Porezag and M. R. Pederson, Phys. Rev. B **54**, 7830 (1996).
[14] K. Witt, Spectrochim. Acta A **24**, 1115 (1968).
[15] L. Cuff and M. Kertesz, J. Phys. Chem. **98**, 12 223 (1994).
[16] S. Guha, W. Graupner, R. Resel, M. Chandrasekhar, H. R. Chandrasekhar, R. Glaser, and G. Leising, J. Phys. Chem. A **105**, 6203 (2001).
[17] M. Ariu, D. G. Lidzey, and D. D. C. Bradley, Synth. Met. **111–112**, 607 (2000).
[18] W. Chunwaschirasiri, B. Tanto, D. L. Huber, and M. J. Winokur, Phys. Rev. Lett. **94**, 107402 (2005).
[19] G. Zerbi, R. Magni, M. Gussoni, K. H. Moritz, A. Bigotto, and S. Dirlikov, J. Chem. Phys. **75**, 3175 (1981).
[20] R. G. Snyder, J. Chem. Phys. **76**, 3921 (1982).
[21] L. Brambilla and G. Zerbi, Macromolecules **38**, 3327 (2005).